의학석사 학위논문

Molecular mechanism of cerebellum-dependent motor learning deficits in *Kdm3b* mutant mouse

Kdm3b 돌연변이 생쥐의 소뇌의존적 운동학습 조절 장애에 대한 분자기전 연구

2019년 8월

서울대학교 대학원

의과학과 생리학전공

김 아 빈

Master's Thesis of Biomedical Science

Kdm3b 돌연변이 생쥐의 소뇌의존적 운동학습 조절 장애에 대한 분자기전 연구

Molecular mechanism of cerebellum-dependent motor learning deficits in *Kdm3b* mutant mouse

August 2019

The Department of Biomedical Science,
Seoul National University
College of Medicine

Ahbin Kim

Abstract

The chromatin remodeling through an epigenetic modification is the fundamental genetic modification through which an individual can adjust to the environmental changes. Histone modification is one of the genetic modifications which modulated by histone methylases and demethylases. Lysine demethylase 3B (KDM3B) is one of the demethylases whole target site is H3K9me2. Cerebellum-dependent motor learning increases H3K9me2 level in the flocculus of wild-type mice. For this purpose, we created *Kdm3b* Het mice to study the function of KDM3B, and its target H3K9me2. Cerebellum-dependent motor learning including OKR increase and VOR increase showed deficits in *Kdm3b* Het mice. In order to confirm these mice having less KDM3B protein amount, immunoblotting analysis was proceeded. Less KDM3B was detected in the flocculus and vermis of *Kdm3b* Het mice compared to wild-type mice. We tested whether this reduced KDM3B amount affects the level of H3K9me2 in the flocculus of cerebellum. However, whole flocculus did not show increased level. Immunohistochemistry indicated that H3K9me2 was expressed in the granule cell layer of the cerebellum vermis specifically. This brain region from *Kdm3b* Het mice was precisely microdissected and immunoblot was performed, showing significantly increased H3K9me2 level in the granule cell, but not in Purkinje cell layer. Granule cell layer of wild-type and *Kdm3b* Het mice were processed to RNA seq. Among the top five Differently Expressed Genes (DEGs) that volume plot analysis represented, *Ncald* and *Etnppl* showed different tendency between *Kdm3b* Het mice compared to the wild-type mice. Moreover, approximately 16000 genes of DEGs, 81 genes passed the standard of significant DEGs. Heatmap and Dendrogram analysis showed that each two members of wild-type groups and two members of *Kdm3b* Het are clustered together. Moreover, some gene levels had been increased in wild-type mice but decreased in *Kdm3b* Het mice. GO analysis displays that Cellular Component GO terms has brain-related terms which would explain the cerebellum-dependent

motor learning deficits. Among three genes, *Ntf3* mRNA level is significantly different between two groups. *Ncald, Etnppl*, and *Ntf3* have known to be related with brain function and disorders. This study demonstrates that epigenetic changes, especially the histone methylation, by KDM3B is associated with cerebellum-dependent motor learning deficit. Moreover, this learning deficit is mediated by several neuronal related genes which specific mechanisms would be further studied.

Keyword : Cerebellum, Histone modification, Demethylase, OKR, *Kdm3b*, Flocculus

Student Number : 2014-25056

초록

에피지노믹 조절에 따른 염색질 재배치는 환경적인 변화에 기반하는 기본적인 유전적 조절이다. 히스톤 조정은 히스톤 메틸레이즈와 히스톤 디메틸레이즈에 의해 변화되는데, Lysine demethylase 3B (KDM3B)는 H3K9me2를 타겟으로 하는 여러 디메틸레이즈 중 하나이다. 흥미롭게도, 소뇌의존적 운동학습인 OKR을 한 후에 OKR 학습과 관련 있는 flocculus wild-type 쥐에서 H3K9me2 레벨이 증가하였다. 이러한 이유로 KDM3B 레벨이 줄어든 *Kdm3b* Hetero 쥐를 제작하여 KDM3B 와 H3K9me2의 역할이 소뇌의존적 운동능력에 미치는 영향을 자세히 연구하고자 하였다. OKR과 VOR 운동학습이 *Kdm3b* Het 쥐에서 망가진 것을 확인하였다. *Kdm3b* Het 쥐에서 실제로 KDM3B가 줄어들었는지 확인하기 위해 웨스턴블랏을 진행하였고 flocculus 영역에서 KDM3B 단백질 발현 양이 줄어들었음을 확인하였다. 그렇다면 줄어든 KDM3B 레벨이 전체 flocculus 에서 H3K9me2 레벨에 영향을 미치는지 확인을 하였지만 레벨 자체에는 영향을 미치지는 않은 것을 확인하였다. IHC 실험을 통해 H3K9me2가 vermis의 granule cell layers에만 특징적으로 발현되는 것을 확인하여 vermis의 granule cell layer와 Purkinje cell layer를 microdissection 하였다. 웨스턴블랏 결과 granule cell 특징적으로 H3K9me2레벨이 *Kdm3b* Het mice에서 증가하는 것으로 확인되었다. 이를 통해 두 종류 쥐의 granule cell layer의 cDNA를 RNA seq을 통해 DEG list를 분석하였다. Volume plot을 통해 top 5 DEGs를 qRT-PCR하여 RNA seq이 유효한지 확인하고자 하였고 *Ncald*와 *Etnppl* 유전자가 DEGs로 나타났다. 약 16000개의 유전자 중에 R 프로그램을 통해 통계적으로 유의미한 DEGs를 걸러내는 기준으로 통과된 유전자는 81개의 유전자였다. 이

유전자로 Heatmap을 그려보았을 때 *Kdm3b* Het mice와 WT mice가 서로 묶이며 DEGs가 나눠지는 것을 확인할 수 있었다. 또한 이 유전자를 Gene Ontology 분석을 통해 나타내었을 때 Cellular Component (CC) GO term에서 뇌 관련 유전자들이 나타난 것을 확인할 수 있었다. 3개의 DEGs 중에 *Ntf3*의 mRNA 레벨이 특정적으로 낮아진 것을 확인하였다. *Ncald, Etnppl, Ntf3*의 총 세개의 뇌 관련 유전자들이 KDM3B를 통한 소뇌의존적 운동학습 조절에 어떻게 영향을 미치는가에 대해서는 후의 연구에서 다뤄야 할 것이다. 이 논문은 에피지노믹 유전인자 KDM3B가 소뇌의 운동능력 조절에 미치는 영향을 분자적 기전 및 transcriptome 기반으로 접근하여 메커니즘을 밝히는데 집중하였다.

주요어: 소뇌, 히스톤 조절, 디메틸레이즈, OKR, *Kdm3b*, Flocculus

Table of Contents

Abstract 1

Abstract in Korean..... 3

Chapter 1. Introduction..... 6

Chapter 2. Meterials & Methods 9

Chapter 3. Results 15

1. Short term learning of optokinetic response increased H3K9me2 level in cerebellar flocculus
2. *Kdm3b* Hetero mice showed lower KDM3B level in cerebellar vermis and flocculus
3. Layer-dependent H3K9me2 changed of vermis in *Kdm3b* Het mice
4. Granule cells of wild-type and *Kdm3b* Het were analyzed by RNA seq
5. DEG expression data between wild-type and *Kdm3b* Het mice sets were analyzed by various statistical methods
6. Gene ontology data set analysis revealed neuron-related GO terms

Chapter 3. Discussion 35

Bibliography 42

Introduction

1.1. Study Background

Chromatin is the complex of compacted DNA associated with protein in the nucleus (Campos and Reinberg 2009). Histone is packed around by DNA which the complex is called by a nucleosome. Histone protein is composed by two H2A-H2B dimers, H3-H4 dimer and one H1 protein associated with linker DNA located between nucleosomes. Depending on how long the linker DNA is, the accessibility of chromatin is determined (Diane E. Handy, Castro, and Loscalzo 2012).

Epigenetic modification refers to the alteration of DNA expression by DNA methylation and histone modification. DNA methylation and histone modification reconstruct chromatin construction and accessibility which regulating patterns of gene expression. Especially, histone methylation patterns and their effects on transcriptions are extremely complex than other epigenetic modification. These modifications are associated with transcriptionally permissive chromatin (euchromatin) and repressive, fostering heterochromatin formation. Importantly, histone methylation marks recruit effector proteins that have important roles in maintaining the transcriptional states of the chromatin. (Diane E. Handy, Castro, and Loscalzo 2012)

Learning and memory formations have two primary concepts which are protein-synthesis independent and time-dependent phase those rely on the activity-induced gene transcription and the protein synthesis (Langmoen and Apuzzo 2007). Epigenetic molecules including chromatin modifications generate and maintain experience-driven behavioral changes in young and old animals. Especially, the epigenetic mechanisms, comprising epigenetic codes, are utilized in long-term memory formations in the adult CNS. (Day and Sweatt 2011)

Lysine demethylase 3b (KDM3B) is a protein coding gene which demethylates

Lysine (K) region of methylation. Representative KDM3B demethylation site is Histone 3 Lysine 9 methylation 2 (H3K9me2) (J.-Y. Kim et al. 2012). H3K9me2 is controlled by several methylases and demethylases which are associated with transcriptional repression(Lachner et al. 2001). KDM3B is epigenetically related to transcriptional regulation. Transcriptional regulation is deeply connected to several cognitive abilities (Bharadwaj et al. 2014), (Cho et al. 2015). Therefore, KDM3B would control memory function and cognitive ability.

Optokinetic response (OKR) is innate eye movement mediated by optic system, which stabilizes images on the retina when the animals move (Liu, Huberman, and Scanziani 2016). OKR composes of a slow-phase and fast-phase eye movement. When one follows a moving object with his eyes and the object move out from the field of vision, one's eyes moves back to the position to the object. This phenomenon is called OKR and this reflex develops around 6 months of age (Okamoto et al. 2011).

The cerebellum-dependent motor learning is focused on the precision and accuracy of ocular movements despite of the head or body movement (Beh, Frohman, and Frohman 2017). Vestibule-ocular reflex (VOR) is a reflex, where activation of the vestibular system causes eye movement. Through detecting head motion and position, and by generating compensatory eye movement, VOR ensures that the angle of gaze remains on target during head motion (Beh, Frohman, and Frohman 2017). The flocculus and the plasticity in Purkinje cells within cerebellar flocculus are associated with VOR (Hansel et al. 2006),(S. J. Kim et al. 2017).

1.2. Purpose of Research

In this paper, we examined whether wild-type mice showed epigenetic changes by OKR learning. Moreover, we made *Kdm3b* Het whole body knock out mice which we assumed that OKR learning would be deficit. We studied how the lack of epigenetic regulation factor of *Kdm3b* Het mice induce cerebellum-dependent

motor learning, which having OKR and VOR dysfunction, mediated by cerebellar flocculus. Moreover, if malfunction of cerebellar motor learning had been appeared, we discovered the mechanism of the change by electrophysiological methods. Plus, we figured out how H3K9me2 level is different after OKR learning and between cerebellar flocculus and vermis. We also dissected granular cell layers and Purkinje cell layers of flocculus and used transcriptome assay in order to find Differentially Expressed Genes (DEGs) between wild-type and *Kdm3b* Het mice. Through using R programming to analyze statistical data, we were able to discover DEGs and Gene Ontology of DEGs. To validate DEGs, qRT-PCR analysis were proceeded and we were able to find cognition-related DEGs. Hence, we were able to figure out the mechanism of KDM3B for controlling cerebellar-dependent motor learning.

Materials and Methods

A. Animals

All animals and experimental procedures described in this thesis were approved by the Institution's Animal Care and Use Committee of Seoul National University College of Medicine. The animals and procedures were also in accordance with the ethical standards of the institutional research committee.

B. Histone purification

In order to extract purified histone protein from tissues, acid and salt extraction were proceeded. Tissues were homogenized with TEB buffer (0.5X triton x-100, 2mM PMSF, 1X Protease inhibitor cocktail) at 4℃ for 30 min. Homogenized tissues were centrifuged by 7000 rpm for 2 minutes at 4℃. After removing the supernatant, pallet was washed with additional TEB buffer and centrifuge in a same condition. After removing soup, 0.5M HCl was added and pipetting was proceeded. The tube was rotated at 4℃ overnight. Tube was centrifuged by 13500 rpm for 10 minutes at 4℃ and the soup was transferred around 90%. 1/3 volume of 100% TCA was added into the tube and the tube was inverted and put in the ice for 2 hours. Occasionally tube was vortexed. Tube was centrifuged by 13500 rpm for 10 minutes at 4℃. The supernatant was removed, acetone was added, and the tube was vortexed. Tube was centrifuged by 13500 rpm for 5 minutes at 4℃. Remove the acetone and repeat the procedure one time. Acetone was air-dried and D.W. was added. The tube was agitated at 4℃ overnight. Tube was centrifuged by 13500 rpm for 5 minutes at 4℃. Collecting the supernatant around 90%.

C. Western blotting

Tissues were homogenized and sonicated with RIPA buffer (25mM Tris-HCl (pH 7.6), 150mM NaCl, 1% NP-40, 1% sodium deoxycholate, 0.1% SDS) with phosphatase inhibitor cocktail and protease inhibitor cocktail. Homogenized soup were centrifuged by 13000 rpm for 15 minutes at 4℃. Supernatant were collected and BCA (Bicinchoninic Acid) analysis was done by using those samples. 3ug of histone or 20ug of brain tissue were used for gel electrophoresis. 5X sample buffer and D.W. were added to histone samples to equalize the volume. Samples were boiled at 95℃ for 5 minutes. 15%, for histone, and 7%, for Kdm3b protein, SDS-polyacrylamide gels were used to separate histone complexes.

Samples were loaded and run at 90V for 3 hours. Histone proteins from gel to PVDF membrane were transferred at 70V for 45 minutes and brain tissues from gel to PVDF membrane were transferred at 25V overnight. Membrane were incubated with primary antibody in 5% BSA-TBST (TBST, TBS + 0.1% triton x-100) overnight. After wash the membranes with TBST 3 time for 10 minutes, membranes were blocked with 2% skim milk for 1 hour and washed 3 times for 10 minutes.

Membranes were exposed to ECL solution (Pierce ECL Western Blotting Substrate, Thermo scientific). Membranes were imaged with digital imager by various timescale (Amersham Imager 600, GE lifescience). Image were stored in JPG and TIFF file format. Protein quantification was performed using AI600 software (GE healthcare), and each band was normalized to α-tubulin or β-actin in the same line.

Primary antibodies and dilution ratios used were below: anti- KDM3B antibody (Cell signaling technology, 2621S, 1:500), anti-H3 antibody (Milipore, 05-499, 1:2000), anti-H3K9me2 antibody (Milipore, 07-441, 1:1000), anti-α-tubulin antibody (Santa cruz, TU-02, 1:2000), anti-β-actin antibody (Santa cruz, AC-15,

1:2000)

D. Immunohistochemistry

Mice were cardiac perfused by PBS and 4% paraformaldehyde. Brains were extracted and put in the 4% paraformaldehyde for one day and subsequent three days in 30% sucrose in PBS. Brains were frozen at -80℃ for a day. By using cryostat, 30μm slices were prepared and stored in a 50% glycerol.

Slices were washed with PBS for 10 minutes by 2 times and PBST with 3% BSA (PBST+) for an hour at room temperature. Slices were incubated with primary antibody diluted with PBST+ for 2 days. On day 3, slices were washed with PBS for 10 minutes by 2 times and PBST+ for an hour. Slices were incubated with secondary antibody diluted with PBST+ for 3 to 4 hours at RT. After incubation, slices were washed with PBS for 5 times at RT, mounted on slice glass, and covered by cover glass.

Primary antibodies used in the IHC are below: anti-calbindin antibody (Abcam, ab82812, 1:500), anti- H3K9me2

E. Microdissection of Vermis tissue slices

Sagittal slices of the cerebellar vermis (250μm) were obtained from wild-type and *Kdm3b* Het mice. Whole regions of the vermis were microdissected into Purkinje neuronal layer (PNL) plus molecular layer (ML) and Granule cell layer (GCL) plus white mater according to the visually detectable borderline. PNL plus ML layer were considered as Purkinje cell layers and GCL plus white matter were considered as Granule cell layers (Ryu et al. 2017).

F. quantitativeRealtime- PCR

Total RNA of Purkinje cell layers and granule cell layers were extracted by using the RNeasy Mini Kit (QIAGEN). Genomic DNA were eliminated by DNase I (QIAGEN) and a total 350μg of RNA was reverse transcribed into cDNA using SuperScript III First-Strand (Invtrogen). qRT-PCR was performed using the CFX connect system (Bio-Rad) with SYBR Premix (TaKaRa). Primers were designed through reference papers or designed by primer-BLAST (https://www.ncbi.nlm.nih.gov/tools/primer-blast). The mRNA expression levels of *Kdm3b* Het mice relative to wild-type were normalized according to the $2^{(-\triangle\triangle Ct)}$ method. All △Ct values were normalized by Ct value of GABRA6 and beta-actin.

G. Statistics

Volume plot analysis

Volume is defined as geometric average between the expression of wild-type and *Kdm3b* Het. Fold change describes how much a quantity changes between the original and subsequent measurements. In order to assess the genes which showed higher volume and which were different between wild-type and *Kdm3b* Het, volume plot was created. X-axis is each gene volume of *Kdm3b* Het over wild-type Y-axis is the log2 absolute fc value. Top five genes were selected by loglfcl>2 and the top 5 highest volumes.

Heatmap and GO analysis

Using FPKM value of each gene was normalized, log2 absolute fold change and raw p-value or each gene of *Kdm3b* Het/WT were used to filter the DEGs. Total 81 genes were survived from this filtering. By using Z-score normalization method.

$$Normalized\ (e_i) = \frac{e_i - \bar{E}}{std(E)} \quad std(E) = \sqrt{\frac{1}{(n-1)}\sum_{i=1}^{n}(e_i - \bar{E})^2} \quad \bar{E} = \frac{1}{n}\sum_{i=1}^{n} e_i \ ,$$

where, e_i is FPKM of each value. Row factors (genotypes) are analyzed by Pearson's correlation, which measure the linear correlation between X and Y. Pearson's correlation coefficient is the covariance of the two variables divided by the product of their standard deviation. Column factors were analyzed by Spearman correlation, which is nonparametric measure of rank correlation by using monotonic function.

After using two analyses, hierarchical clustering was used for gene clustering method. Hierarchical clustering starts by treating each observation as separate cluster. After identifying the two clusters that are closest together, it merges the two most similar clusters. This continues until all the cluster are merge together. The methods described above was used for Heatmap and Dendrogram drawing by coding R programming.

Cutree function in R, which cuts the Dendrogram at specific height and clusters divided group together, was proceeded for grouping DEGs. Total 5 groups of DEGs were created (Cutree = 4). Biological Process (BP), Molecular Function (MF), and Cellular Component (CC) GO of gene set were examined and confirmed by PANTHER Gene List Analysis (http://pantherdb.org/tools/index.jsp). They were described at right side of the heat map.

Gene Ontology (GO) network of each 81 gene set was analyzed by ClueGO (Bindea et al. 2009). Gene set enrichment analysis network were plotted and bar graphs which present the percentage of associated genes and absolute gene numbers included were plotted. Pathways with pV (term p value corrected with Bonferroni step down) ≤ 0.05 were marked with asterisk in each bar.

Other statistics methods

A statistical method used in western blotting and qPCR was quantified by Prism 7.

Parametric unpaired t-test followed by two-tailed p value (statistically significant when $p \leq 0.05$) was calculated.

Results

1. Short term learning of optokinetic response increased H3K9me2 level in cerebellar flocculus

Wild-type mice ran through OKR learning and after 1hr, brain proteins were extracted. Cerebellar flocculus and vermis were dissected and histone extracts were created. Home cage group and 1 hour after OKR learning group histone extracts were western blotted. H3K9me2 and H3 level were measured (figure. 1). Total 3 batches of experiments were proceeded and the results of 1st and 3rd batch were used. When the data of 1st and 3rd batch were put together, there was significant increase of H3K9me2 level after 1hr of OKR learning (figure. 1).

2. *Kdm3b* Hetero mice showed lower KDM3B level in cerebellar vermis and flocculus

As this experiment showed that OKR learning affected H3K9me2 level which would be regulated by KDM3B, we created *Kdm3B* Hetero mice having learning deficit. Western blot of cerebellar flocculus and vermis brain extracts have been proceeded. KDM3B, a-tubulin and b-actin antibodies were attached to membrane. KDM3B level was measured in WT and *Kdm3B* Het. About 40% of KDM3B protein level was reduced, which ensured that *Kdm3b* Het mice have less KDM3B protein level (figure.2).

3. Layer-dependent H3K9me2 changed of vermis in Kdm3b Het mice

In this paper, we did not show the result, but previous experiment of OKR and VOR behavior test have been done. OKR increase and VOR increase were malfunctioned, but VOR decrease was normal in *Kdm3b* Het mice. Whether this

behavioral changes were affected by H3K9me2, we measured H3K9me2/H3 level in *Kdm3b* Het flocculus histone extracts. There is no difference H3K9me2/H3 level between two groups (figure. 3).

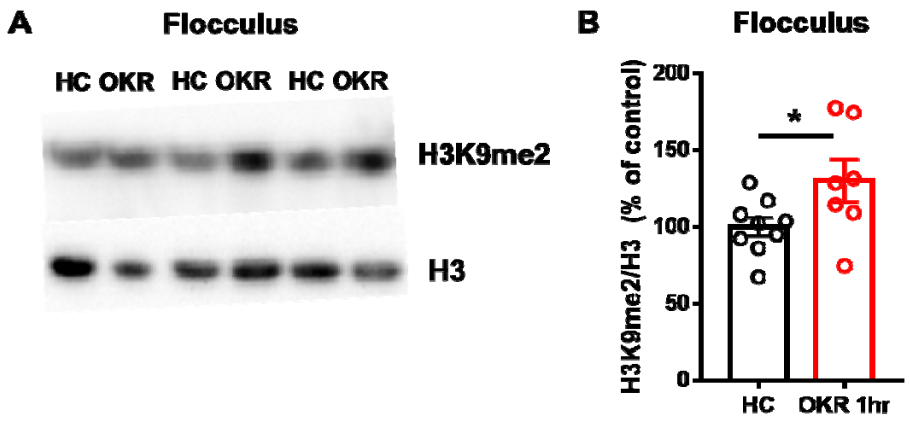

Figure 1 Increased Level of Histone Methylation in Wild-type Mice of One Hour after Optokinetic response (OKR) Learning Compared to Homecage. (A) Western blot of H3K9me2 and H3 in Histone extract of homecage and OKR learning mice first batch. homecage; n=4, OKR; n=3. (B) WB quantification of (A). H3K9me2/H3 level was measured. Unpaired t-test; p=0.0087. Each dot represents one sample. 1st, 3rd batch; HC, n=5, OKR, n=5.

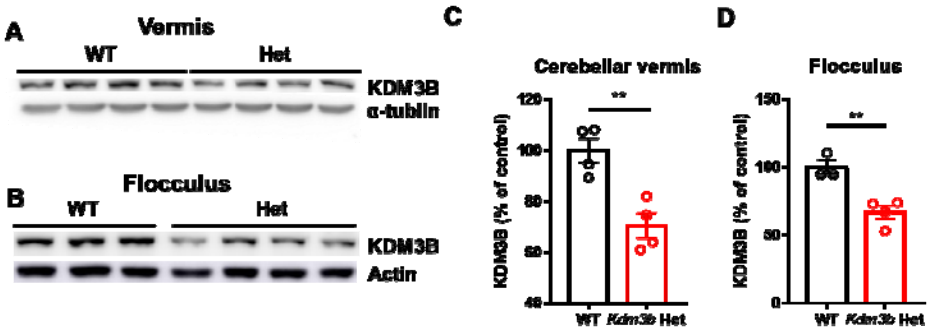

Figure 2 Lower KDM3B Level in both Vermis and Flocculus of *Kdm3b* Hetero Mice. (A) Western blot of Kdm3b and a-tubulin in cerebellar vermis of WT and *Kdm3b* Het mice. (C) Quantification of WB; Unpaired t-test, p=0.0048, WT, n=5, *Kdm3b* Het, n=5. (B) Western blot of KDM3B and beta-actin in the flocculus. (D) Quantification of WB; Unpaired t-test, p=0.0059, WT, n=3, Het, n=4

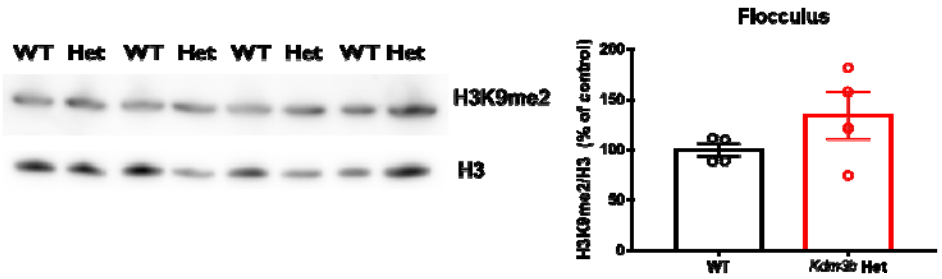

Figure 3 H3K9me2/H3 Level of Flocculus in WT and *Kdm3b* Het Mice. (A) Western blot of H3K9me2 and H3 level in histone extract of WT and *Kdm3b* Het mice. (B) WB Quantification of H3K9me2/H3 of flocculus in WT and Kdm3b Het. WT, n=4, Het, n=4, Unpaired t-test, two-tailed, p=0.2086 (non-significant)

In order to see H3K9me2/H3 level through Immunohistochemistry (IHC) in WT cerebellum, we have been done staining of vermis and flocculus. CALBINDIN, which emission light is green, stained Purkinje cells specifically and KDM3B, which emission light is red, stained granule cells specifically (figure. 4. A). To confirm layer specificity of Kdm3B in wild-type and *Kdm3b* Het mice, we micro dissected vermis granule cells and Purkinje cells (figure.4. B, C). Histone extracts of these layers were western blotted and H3K9me2/H3 level was measured. About 60% increase of H3K9me2/H3 observed in *Kdm3b* Het granule cell layers compared to wild-type granule cell layers. On the other hand, there was no difference in H3K9me2/H3 level between Purkinje cell layers between two mouse groups (figure. 4. D, E).

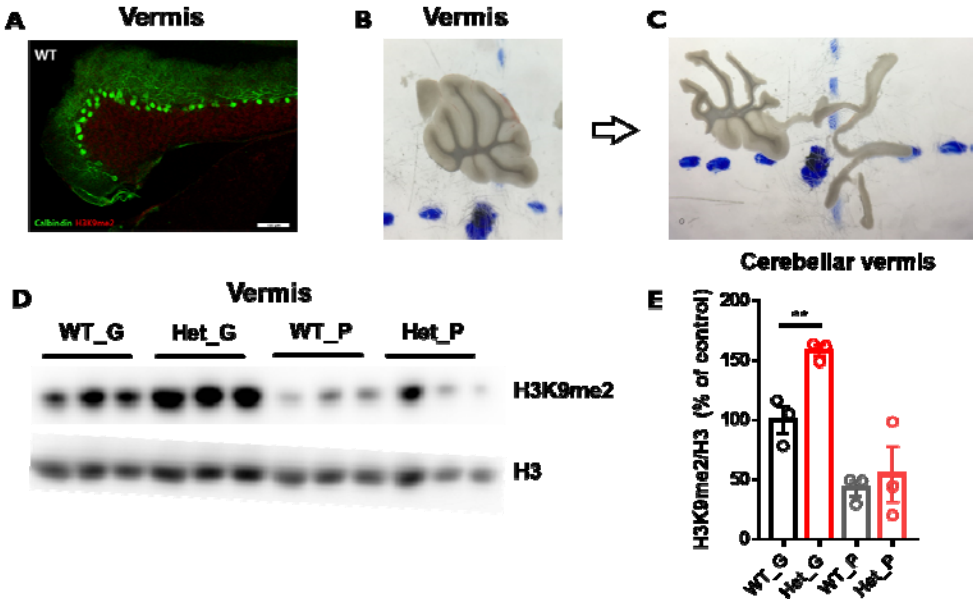

Figure 4 Layer-specific H3K9me2 Expression of Cerebellar Vermis in Wild-type and *Kdm3b* Het Mice. (A) Immunohistochemistry (IHC) of cerebellar vermis. CALBINDIN was stained as green, while H3K9me2 was stained as red color. Scale bar; 100um. * This data is obtained done by Myeong Seong Bak. (B) Layer-specific microdissection of cerebellar vermis. Granule cells and Purkinje cells were divided into two and each section was processed into histone extracts. ¶ This experiment is done by Yong Gyu Kim. (C) Western blot of cerebellar vermis granule cells and Purkinje cells histone extracts. H3K9me2 and H3 were measured. (D), (E) WB quantification of (C) each group; n=3, WT_Granule vs Het_Granule, unpaired t-test; p=0.0088.

4. Granule cells of wild-type and Kdm3b Het were analyzed by RNA seq

Since histone methylation level was different between two groups, we decided to extract layer-specific RNA from vermis granule and Purkinje cell layers. We first confirmed that these RNA extracts were layer-specific. *Pcp* is Purkinje cell layer-specific gene and *Gabra6* is granule cell layer-specific gene. qPCR experiment was qualified as Cq values were similar in all groups (figure. 5. A). Only *Pcp* gene appeared in wild-type and *Kdm3B* Het granule cell layers an*d Gabr*a6 gene appeared in wild-type and *Kdm3B* Het Purkinje cell layers (figure. 5. B, C). The sizes of actin, *Pcp* and *Gabra6* were appeared in the 2% agarose gel (figure. 5. D)

Vermis granule cell layers of wild-type and *Kdm3b* Het mice were analyzed for RNA seq. RNA seq was proceeded using two wild-type and two *Kdm3b* Het mice and various data mining has been produced. Expression profile of a numerous genes and each gene FPKM (Fragments Per Kilobase Million) value was given. Z-score normalization was necessary in order to reduce the distribution of data. Over 1.5 of Fold change and under 0.05 of raw p-value of genes were used. 81 genes over 16447 genes were selected

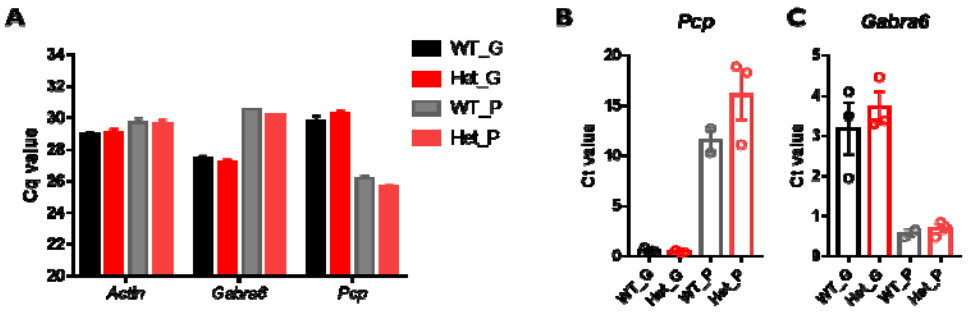

Figure 5 Layer-specific RNA Extraction of Cerebellar Vermis in Wild-type and *Kdm3b* Het. (A) qPCR result of Cq Values*: Actin, Gabra6* and *Pcp*. (B, C) Relative RNA levels of *Pcp* and *Gabra6* in each sample

5. DEG expression data between wild-type and *Kdm3b* Het mice sets were analyzed by various statistical methods

Volume plot x-axis represents the volume, which is the expression of wild-type divided by *Kdm3b* Het. Y-axis is log2 of absolute value fold change of FPKM value. Top five statistically significant genes are listed below: *Rpph1, Vps26a, Ncald, Gpx3, Etnppl*. These genes were used to qualify RNA seq data. We produced primers of these genes and qRT-PCR experiment was proceeded. Since H3K9me2 level of granule cell layer were different between two mouse groups, we used granule cell cDNA to qRT-PCR analysis (figure. 6). Among five of them, *Ncald* mRNA level was not significant, but had a tendency and *Etnppl* mRNA level was not significant, but had a strong tendency between wild-type and *Kdm3b* Het mice (figure.7)".

R studio program was used for gene set clustering analysis. Hierarchical clustering method, after Pearson's and Spearman correlation, was used for Heatmap and Dendrogram drawing. Cutree function was proceeded for dividing groups of DEGs. Total five groups of DEGs were created (Cutree = 4). Gene ontology (GO) of each gene set was analyzed by ClueGO (Bindea et al. 2009). Biological Process (BP), Molecular Function (MF), and Cellular Component (CC) GO of gene set were examined.

As a result of the clustering, GOs of each group was not related to a neuron or synapse. CC GO terms showed that Cytoplasmic Part and Endomembrane Part were appeared. BP GOs terms showed that the Response to External Toxic Stimulus, Immune System, Nucleobase-containing Compound Metabolic Process, and Regulation of Biological Quality were exhibited. MF GOs were Cation Binding, Hydrolase Activity, and Anion Binding (figure. 8).

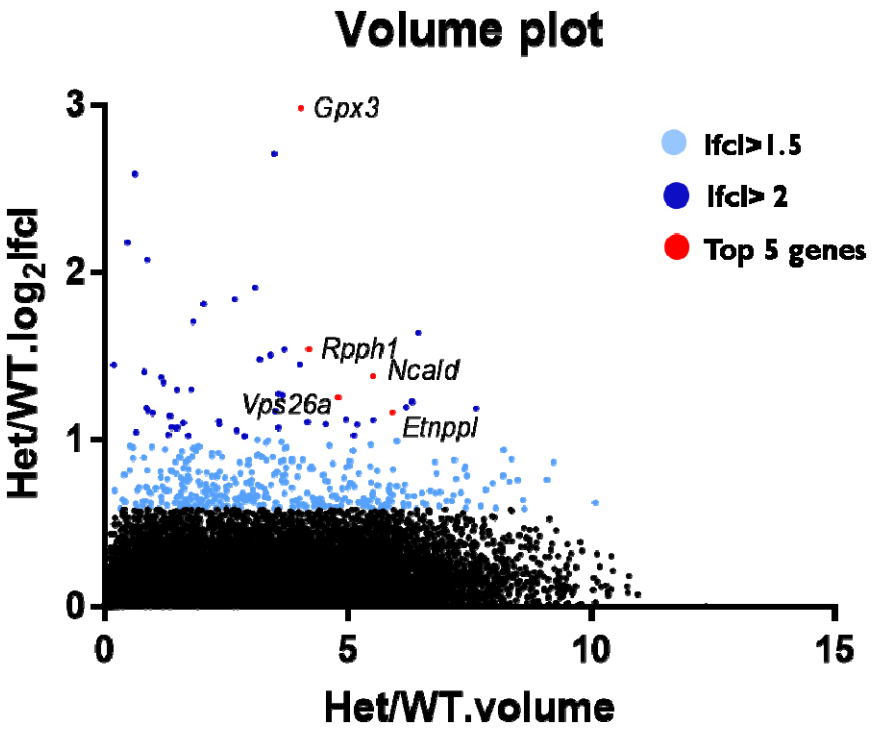

Figure 6 Volume Plot between Wild-type and *Kdm3b* Het. Volume is defined as a geometric average between the expression of wild-type and *Kdm3b* Het. Volume plot x axis is volume and y axis is log2 of fold change. Red dots represent IfcI>=2 & independent T-test raw p-value<0.05. Top five ranking genes of volume are red dots.

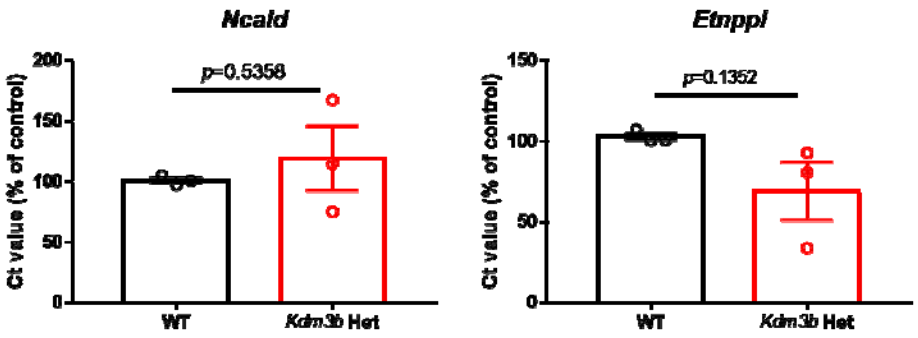

Figure 7 qRT-PCR Validation of RNA Seq Data Analyzed by Volume Plot. mRNA levels of (A) *Ncald* and (B) *Etnppl* were measured by quantitative Real Time-PCR. Ct value is $2^{(-\triangle\triangle Ct)}$. n=3 for each group. Unpaired t-test, *Ncald*; p=0.5358 (non-significant), *Etnppl*; p=0.1352 (non-significant).

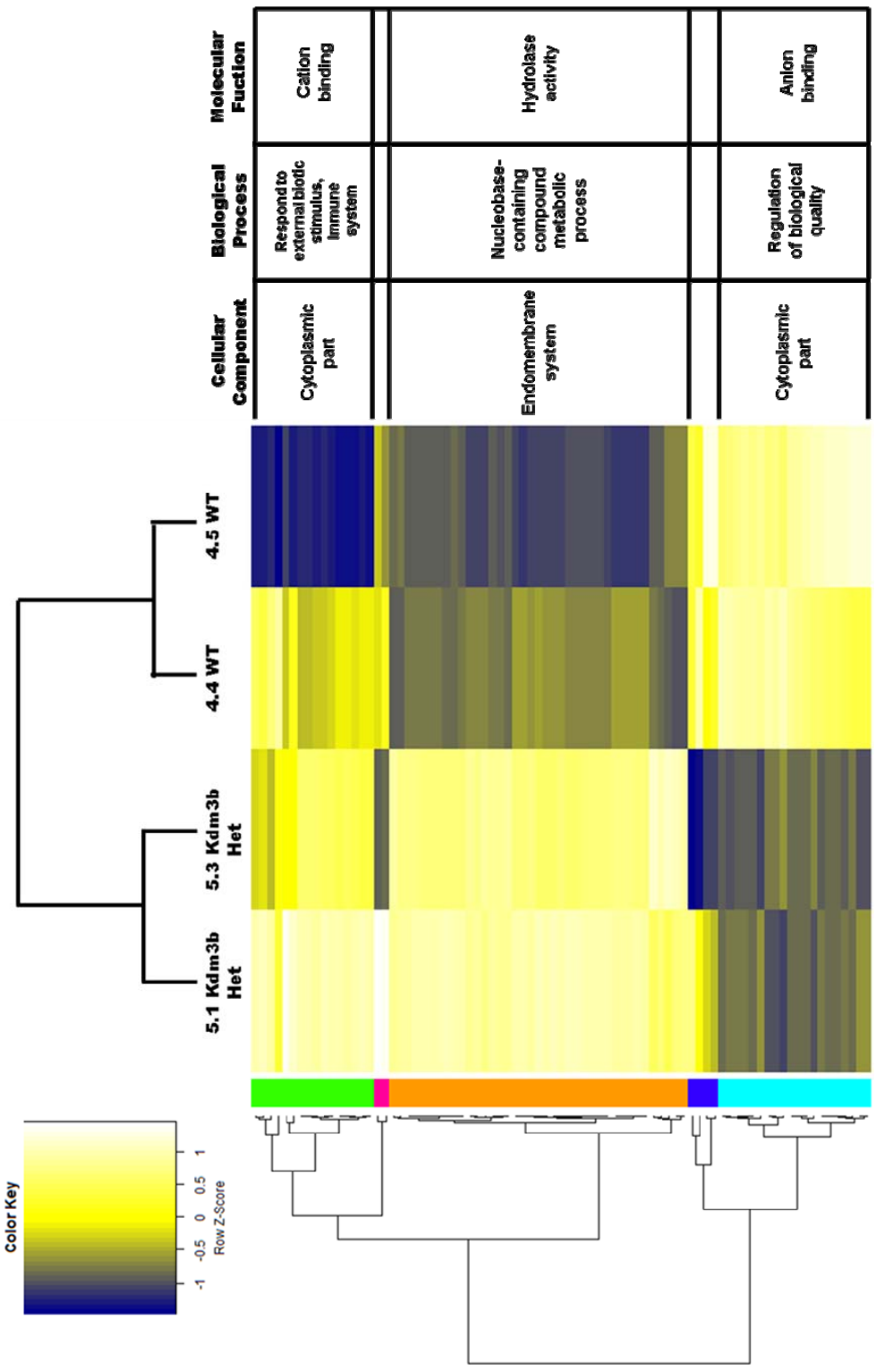
Molecular Fuction
Biological Process
Cellular Component
Cation binding
Hydrolase activity
Anion binding
Respond to external biotic stimulus, immune system
Nucleobase-containing compound metabolic process
Regulation of biological quality
Cytoplasmic part
Endomembrane system
Cytoplasmic part
4.5 WT
4.4 WT
5.3 Kdm3b Het
5.1 Kdm3b Het
Color Key
Row Z-Score
-1
-0.5
0
0.5
1

Figure 8 Heat Map of One-way Hierarchical Clustering and BP, MF, CC of DEGs. WT and *Kdm3b* Het RNA extracts were used for RNA seq. DEG list were extracted by Z-score based FPKM normalized values (Hierarchical clustering analysis, Euclidean distance, Complete linkage). DEGs are divided into 5 groups by specific height (h=4) of Dendrogram. BP (Biological Process), MF (Molecular Function), and CC (Cellular Component) of each group are listed at the right boxes.

6. Gene ontology data set analysis revealed neuron-related GO term

When top 81 genes were GO analyzed simultaneously, different results were revealed. As a result of our data, the largest percentage of gene BP GO is Positive Regulation of Cell Adhesion, followed by the Response to Molecule of Bacterial Origin and the Negative Regulation of Locomotion. The largest percentage of gene CC GO is Mitochondrion, followed by Intracellular Vesicles, Plasma Membrane, and Cell Surface. Furthermore, MF GOs were divided into two identical portions; Cysteine-type Peptidase Activity and Tubulin Binding.

Focused on Cell Surface GO in CC, this term includes Neuron Part and Neuron Projection. By extracting the gene list of Cell Surface GO, we made ten DEG candidates primers to identify which genes influence *Kdm3b* Het cerebellum-dependent motor learning deficit. These genes included several neuronal related genes such as *Etnppl* (Ding et al. 2016), *Ntf3* (Wan et al. 2014), *Calb1* (Ryu et al. 2017), and *Camk2b* (Waggener et al. 2013).

We would like to know which gene is related to the deficit of cerebellum-dependent motor learning. We found qRT-PCR primers of these genes through the papers. qPCR analysis asserted that *Ntf3* gene is downregulated in *Kdm3b* Het mice (figure. 12).

To sum up, OKR one-hour learning changed H3K9me2 level, which is thought to be one of the action sites for KDM3B protein. To understand the importance of KDM3B in cerebellum-dependent motor learning, we created *Kdm3b* Het mice. *Kdm3b* Het mice have relatively low KDM3B protein levels in flocculus and vermis tissues. H3K9me2 level did not show any change in whole flocculus. In granule cell layers, *Kdm3b* Het mice have higher H3K9me2 level compared to wild-type mice. On the other hand, Purkinje cell layer showed no difference between two groups. We did RNA seq for granule cell lines of two groups. The standard of DEGs used from DEG list given by company is lfcl <2 and raw $p<0.05$.

First of all, we selected 5 genes from the volume plot. Among 5 genes, *Ncald* and *Etnppl* showed changed RNA quantity in *Kdm3b* Het mice proved by quantitative RT-PCR. We did GO analysis for 81 genes which passed the standard, and only in CC GO, Neuron Part and Neuron-related Part came out. We did qRT- PCR for these genes and *Ntf3* gene was differentially expressed in *Kdm3b* Het mice. We estimated that the genes such as *Ncald, Etnppl*, and *Ntf3* affected the KDM3B-mediated deficit of cerebellum-dependent motor learning.

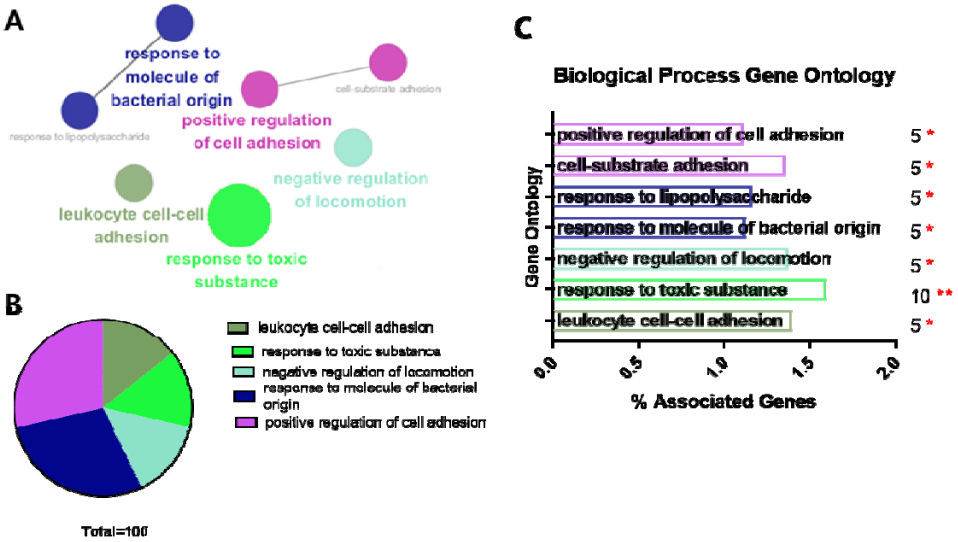

Figure 10 Top 81 Enriched Gene Ontology Biological Process (BP) in Wild-type versus *Kdm3b* Het Mice. The list of DEGs detected by RNA-Seq was investigated for significantly ($p<0.05$) enriched Biological Process (BP) using ClueGO Biological Process (BP) tool. (A) BP of GO enrichment network. Representative components of network are labeled as bold. (B) Pie chart of GO percent terms per group. (terms associated with the group / total terms found * 100) Colors reflect the degree of connectivity between terms based on the network. (C) All enriched BP were ranked from top to bottom based on the p-values for each GO term. Bars represent the percentage of associated genes found in wild-type versus those found in *Kdm3b* Het. Absolute numbers of associated genes are depicted at the end of the bars. Term p-value (corrected by Bonferroni step down) ≤ 0.05 is marked as an asterisk

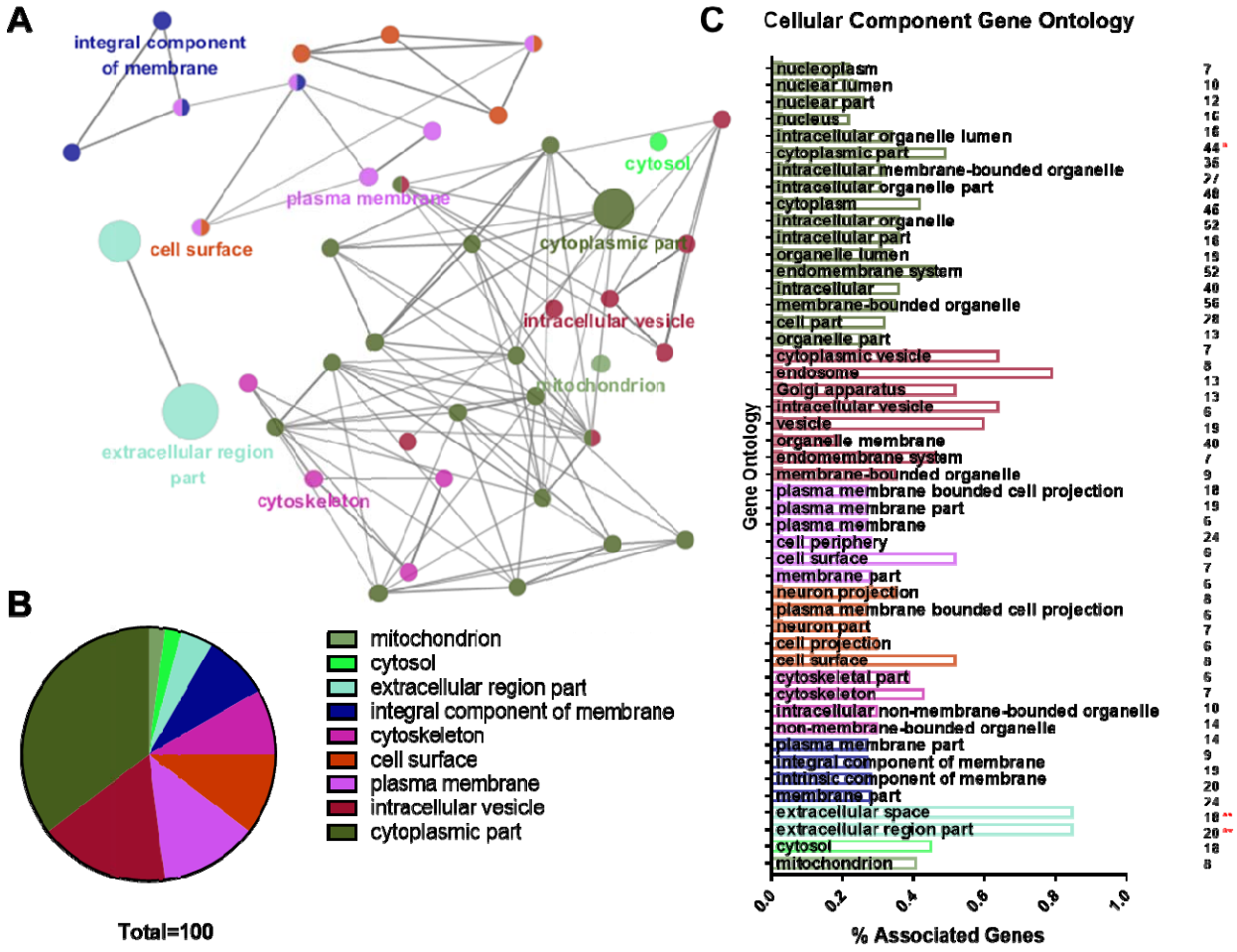
A
integral component of membrane
plasma membrane
cytosol
cell surface
cytoplasmic part
intracellular vesicle
mitochondrion
extracellular region part
cytoskeleton
B
mitochondrion
cytosol
extracellular region part
integral component of membrane
cytoskeleton
cell surface
plasma membrane
intracellular vesicle
cytoplasmic part
Total=100
C
Cellular Component Gene Ontology
Gene Ontology
nucleoplasm 7
nuclear lumen 10
nuclear part 12
nucleus 16
intracellular organelle lumen 16
cytoplasmic part 44 *
intracellular membrane-bounded organelle 36
intracellular organelle part 37
cytoplasm 48
intracellular organelle 46
intracellular part 52
organelle lumen 16
endomembrane system 15
intracellular 52
membrane-bounded organelle 40
cell part 56
organelle part 28
cytoplasmic vesicle 13
endosome 7
Golgi apparatus 8
intracellular vesicle 13
vesicle 13
organelle membrane 6
endomembrane system 19
membrane-bounded organelle 40
plasma membrane bounded cell projection 7
plasma membrane part 9
plasma membrane 18
cell periphery 19
cell surface 6
membrane part 24
neuron projection 6
plasma membrane bounded cell projection 7
neuron part 8
cell projection 6
cell surface 7
cytoskeletal part 6
cytoskeleton 8
intracellular non-membrane-bounded organelle 6
non-membrane-bounded organelle 7
plasma membrane part 6
integral component of membrane 10
intrinsic component of membrane 14
membrane part 14
extracellular space 9
extracellular region part 19
cytosol 20
mitochondrion 24
18 **
20 **
18
8
0.0
0.2
0.4
0.6
0.8
1.0
% Associated Genes

Figure 10 Top 81 Enriched Gene Ontology Cellular Component (CC) in Wild-type versus *Kdm3b* Het Mice. The list of DEGs detected by RNA-Seq was investigated for significantly ($p<0.05$) enriched Cellular Component (CC) using ClueGO Cellular Component (CC) tool. (A) CC of GO enrichment network. Representative components of network are labeled as bold. (B) Pie chart of GO percent terms per group. (terms associated with the group / total terms found * 100) Colors reflect the degree of connectivity between terms based on the network. (C) All enriched CC were ranked from top to bottom based on the p-values for each GO term. Bars represent the percentage of associated genes found in wild-type versus those found in *Kdm3b* Het. Absolute numbers of associated genes are depicted at the end of the bars. Term p-value (corrected by Bonferroni step down) ≤0.05 is marked as an asterisk

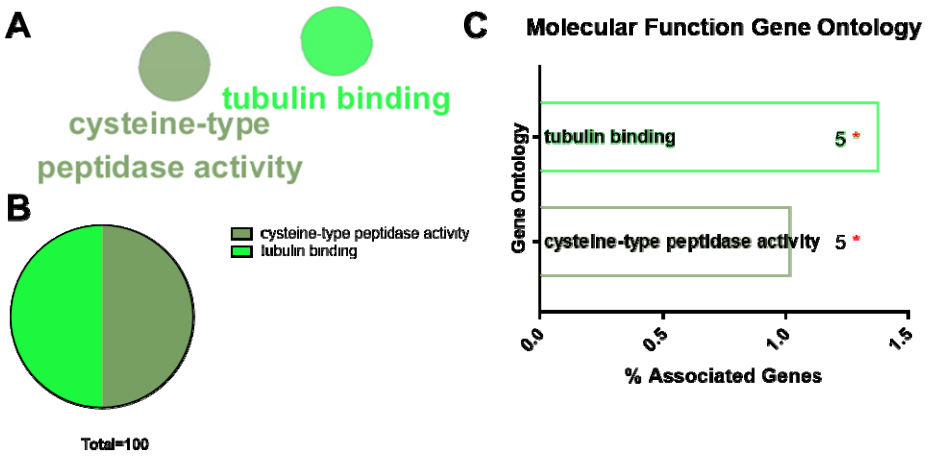

Figure 11 Top 81 Enriched Gene Ontology Molecular Function (MF) in WT versus *Kdm3b* Het Mice. The list of DEGs detected by RNA-Seq was investigated for significantly ($p<0.05$) enriched Molecular Function (MF) using ClueGO Molecular Function (MF) tool. (A) MF of GO enrichment network. Representative components of network are labeled as bold. (B) Pie chart of GO percent terms per group. (terms associated with the group / total terms found * 100) Colors reflect the degree of connectivity between terms based on the network. (C) All enriched MF were ranked from top to bottom based on the p-values for each GO term. Bars represent the percentage of associated genes found in wild-type versus those found in *Kdm3b* Het. Absolute numbers of associated genes are depicted at the end of the bars. Term p-value (corrected by Bonferroni step down) ≤0.05 is marked as an asterisk

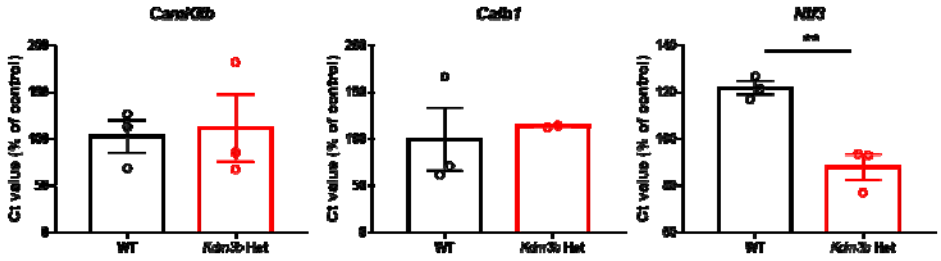

Figure 12 qRT-PCR of Three Candidate Genes from Cell Surface Gene Ontology Including Neuron Part and Neuron Projection. Three candidate genes from Cell Surface GO are listed and qRT-PCR analysis was proceeded. *CamKIIb* and *Calb1* mRNA levels were not changed between wild-type and *Kdm3b* Het mice. *Ntf3* mRNA level was significantly changed between two groups ($p<0.0001$). WT, n=3; TG, n=3.

Discussion

To summarize, cerebellum-dependent OKR learning increases H3K9me2 level in wild-type mice flocculus (figure. 1). This elevation is related to the structural regulation of a chromatin, especially during the creation of a heterochromatin in the nucleosome. Thus, related transcriptional regulation factors are not able to access targeted DNA, which results in the suppression of gene transcription.

The rationale behind creating *Kdm3b* Het mice is inscribed as following: 1) H3K9me2/H3 level was increased in wild-type OKR learning group and 2) cerebellum-dependent memory deficit would be caused by the reduction of the histone demethylase. We chose KDM3B as a specific demethylase for H3K9me2 site since KDM3B is known to demethylate H3K9me2 and repress the transcriptional activation.

How this repression of gene transcription affects memory deficits in cerebellum-dependent motor learning? It is generally accepted that long-term potentiation (LTP) requires the protein synthesis, including ERK and NMDAR (Lu and Malenka 2012) (Scharf et al. 2017). It is also known that an increased H3K9me2 level in the lateral amygdala (LA) was identified at 1 hour following auditory fear conditioning (Gupta-Agarwal et al. 2014). Moreover, this action was largely regulated by GluN2B-containing NMDARs via ERK activation, which are critical in LTP formation. Similarly, Repression of KDM3B activity followed by the molecular-conformational change in H3K9me2 would influence motor learning in cerebellum by reducing LTP formation.

We created *Kdm3b* Het mice and confirmed that KDM3B protein level is decreased in both flocculus and vermis of this genetically mutant mice (figure.2). Additionally, The OKR increase behavior and VOR increase behavior deficits appeared in *Kdm3b* Het mice. To sum up, cerebellum-dependent motor learning deficit of *Kdm3b* Het mice would be apparent by decreased KDM3B level

Another experiment that should have been done was comparing KDM3B level in

Wild-type mice before and 1-hour after OKR learning (figure. 1). We do not have primary evidence that changed H3K9me2 level in flocculus was caused by KDM3B. If the RNA or protein expression level was changed, we can easily estimate that KDM3B affected H3K9me2 level and consequently, the cerebellum-dependent motor learning.

It can be also assumed that the remodeling of a chromatin by KDM3B demethylase change the behavioral phenotype of *Kdm3b* Het mice. In order to demonstrate this hypothesis, we compared H3K9me2 level in whole flocculus of wild-type and *Kdm3b* Het mice. However, H3K9me2 levels were not different between two groups (figure.3). It can be assumed that as H3K9me2 site is controlled by various methylases and demethylases, the action of KDM3B would be masked by other transcriptional regulator.

There is another possibility that the exact moment when histones were extracted from the mouse flocculus would not be a proper time point. Histones were extracted from wild-type and KDM3B mice which showed distinct phenotypical changes after the cerebellum-dependent learning.

Immunostaining of wild-type mouse cerebellum vermis showed the specific expression of KDM3B in the granule cell layers. This specific KDM3B expression is indicated by KDM3B not overlapping with CALBINDIN1, Purkinje cell marker (figure. 4A). To verify this issue, microdissection of vermis had been performed (figure. 4B, C). Surprisingly, H3K9me2 level in granule cell layer of *Kdm3b* Het mice was significantly higher than wild-type mice, but that of Purkinje cell layer was not different between two groups (figure. 4D, E).

Due to its developmentally limited size, layer specific H3K9me2 level in the cerebellum flocculus was absurd to achieve. However, cerebellum was well known for its relatively uniform anatomical structure. Hence, we could assume that using cerebellum vermis, instead of flocculus, for layer specific microdissection would give us a consistent result. We proclaim that we used cerebellum vermis granule cells instead of flocculus granule cells, as this surmise has been applied to all

following experiments.

Electrophysiological result, which is not shown in this paper, states that Purkinje cells, which are the postsynaptic neuron of granule cells, showed lower frequency in spontaneous EPSCs and longer inter-spike interval. From this circumstance, we can assume that there were molecular synthesis events in the granule cell layers. Presumably, anonymous protein synthesis would cause the firing rate of Purkinje cells lowering frequency. Therefore, we concluded that increased H3K9me2/H3 level by decreased KDM3B would mediate granule cell epigenetic change and this gene modification subsequently affects the electrophysiological characteristic of Purkinje cells.

With regard to the difference in granule cell levels, we did RNA seq analysis using cerebellum vermis granule cell layer. About 16000 DEGs were identified. Volume plot was created, while top 5 genes were proceeded through qRT-PCR. Both *Ncald* and *Etnppl* RNA levels were significantly different between wild-type and *Kdm3b* Het mice.

Ncald is a neuronal calcium sensor and a Ca2+-dependent negative regulator of endocytosis (Riessland et al. 2017). This gene reduction acts protective against spinal muscular atrophy (SMA) (Riessland et al. 2017). However, a complete of *Ncald* impairs adult neurogenesis (Upadhyay et al. 2019). On the other hand, *Ncald* overexpression decreases the number of dendrite in cultured neurons (Yamatani et al. 2010). In *Kdm3b* Het mice, *Ncald* RNA level was higher than wild-type mice. This elevated NCALD might affect the deficit of cerebellum-dependent motor learning by decreased dendritic morphology in the cerebellum.

It is known that cerebellum has been related to psychiatric disorder such as attention deficit hyperactivity disorder (ADHD), autism spectrum disorder (ASD), and bipolar disorder (BD) (Phillips et al. 2015). An impairment of cerebellum can implicate such manifold psychiatric disorders as this brain region is connected to the cerebral cortex, including frontal cortex, motor cortex and parietal cortex.

ETNPPL protein has a putative mitochondrial subcellular localization and

expressed only brain relevant library. This gene is also related to bipolar disorder and schizophrenia (Shao and Vawter 2008). We can assume that ETNPPL downlegulation in *Kdm3b* Het mice leads to the impairment of cortico-ponto-cerebellar pathway and cerebello-thalamo-cortical pathway. Decreased cerebellar ETNPPL level means deficit of cerebellar-cortical circuit, which would affect cerebellum-dependent motor function (Shao and Vawter 2008). Therefore, these neuronal system-related two genes would have putative roles in deficits of *Kdm3b* Het mice having cerebellar motor learning function.

Genes that are passed through the standard (lfcl >1.5, raw p-value ≤ 0.05) of gene filtering of significance test were used for further data analysis. *Kdm3b* Het and wild-type mice showed DEGs that were grouped together demonstrated in the Heatmap and Dendrogram. Nevertheless, there is a subtle difference within a group. The number of samples that we sent for RNA seq was two for each group. So that could be the reason why there are dissimilarities within each group. Moreover, granule cell layer would not be purely separated when the cerebellum vermis is microdissected. These problems would cause the intra-group differences within the Heatmap.

Gene Ontology (GO) analysis was done by several programmatic tools and revealed that in Biological Process and Molecular Function, there are no brain-related GO terms. Although it is not significant as group term p-value score, there are neuronal related term in Cellular Component GO term such as Neuron Part, Cell Projection, and Plasma Membrane Cell Bounded. This brain-related GO term groups mean that the cerebellum-dependent learning deficits would be the gene from this DEGs.

We picked a few genes from neuronal related terms; *CamKIIb* (Ca2+/calmodulin-dependent protein kinase II b), *Calb1* (Calbindin 1), and *Ntf3* (Neurotrophin 3). By qRT-PCR analysis, mRNA level of each gene was measured. Among those gene candidates, *Ntf3* gene is the only gene which mRNA level was significantly different between two groups.

NTF3 is a neurotrophin factor that is essential for the generation of long-lasting new synaptic connection (Huang and Reichardt 2001). A number of studies indicate that NTF3 produces a rapid increases in synaptic strength within nerve-muscle synapses, as well as an increase in excitatory post-synaptic currents (EPSC) in hippocampal neurons (Lohof, Ip, and Poo 1993), (Kang H and Schuman EM. 1995), (Levine et al. 1995). Moreover, NTF3 produces rapid and long-lasting enhancement of synaptic strength through LTP in hippocampal slice. Moreover, the research regard cerebellum and NTF3 is still ongoing (Segal et al. 1995) (Sadakata et al. 2014) (Xu and Sajdel-sulkowska 2013). Most of them demonstrate that cerebellar NTF3 has an effect on granule cell layers' development.

In our case, *Kdm3b* Het mice showed less amount of *Ntf3* mRNA in cerebellum granule cell layers when analyzed by qRT-PCR. Reduced Ntf3 mRNA level in *Kdm3b* Het would be related to the weakened synaptic strength in cerebellar connection or the developmental deficit of cerebellar granule cell layers. These deficiencies would be the source of dysfunction in cerebellum-dependent motor learning deficits.

Moreover, as KDM3B protein is declined, whole transcriptome or the levels of specific proteins would be changed during learning stage. This change would affect the process of memory formation or memory consolidation which ultimately influence deficits in cerebellum-dependent OKR learning. For this purpose, the experiments below need to be performed.

H3K9me2 level before and after OKR learning in *Kdm3b* Het mice has not been measured. If measured, this can be a key data as it elucidates the relationship between KDM3B and cerebellum-dependent motor learning while OKR learning is proceeded.

KDM3B level and *Kdm3b* mRNA level before and after OKR learning in wild-type mice and *Kdm3b* Het mice has not been measured. We can estimate that KDM3B function for OKR and VOR *in vivo* in both group mice directly if this data exists.

Kdm3b is a candidate gene for Wilms tumor, which is the most common childhood renal cancer (Mahamdallie et al. 2019). Recently, a study identified epigenetic genes that related to schizophrenia by cross-referencing with GWAS loci. It revealed that one of the Schizophrenia risk genes is *Kdm3b* (Whitton et al. 2016).

Our research firstly demonstrates that an epigenetic factor KDM3B protein is associated with the working memory of cerebellum. KDM3B acts on the site of H3K9me2 and changes the density of chromosome, altering the transcription level of specific genes. Possible neuronal candidate genes have been suggested: *Ncald, Etnppl*, and *Ntf3*. Overall, our study proposes that epigenetic changes is crucial for cerebellum-dependent motor learning.

Bibliography

Beh, Shin C., Teresa C. Frohman, and Elliot M. Frohman. 2017. "Cerebellar Control of Eye Movements." *Journal of Neuro-Ophthalmology* 37(1): 87–98.

Bharadwaj, Rahul et al. 2014. "Conserved Higher-Order Chromatin Regulates NMDA Receptor Gene Expression and Cognition." *Neuron* 84(5): 997–1008. http://dx.doi.org/10.1016/j.neuron.2014.10.032.

Bindea, Gabriela et al. 2009. "ClueGO: A Cytoscape Plug-in to Decipher Functionally Grouped Gene Ontology and Pathway Annotation Networks." *Bioinformatics* 25(8): 1091–93.

Campos, Eric I., and Danny Reinberg. 2009. "Histones: Annotating Chromatin." *Annual Review of Genetics* 43(1): 559–99. http://www.annualreviews.org/doi/10.1146/annurev.genet.032608.103928.

Cho, Seo-Hyun et al. 2015. "SIRT1 Deficiency in Microglia Contributes to Cognitive Decline in Aging and Neurodegeneration via Epigenetic Regulation of IL-1b." *J Neurosci* 35(2): 807–18.

Dalvi, Maithili P et al. 2017. "Taxane-Platin-Resistant Lung Cancers Co-Develop Hypersensitivity to JumonjiC Demethylase Inhibitors." *Cell Reports* 19(8): 1669–84. http://dx.doi.org/10.1016/j.celrep.2017.04.077.

Day, Jeremy J., and J. David Sweatt. 2011. "Epigenetic Mechanisms in Cognition." *Neuron* 70(5): 813–29. http://dx.doi.org/10.1016/j.neuron.2011.05.019.

Diane E. Handy, Rita Castro, and Joseph Loscalzo. 2012. "Epigenetic Modifications: Basic Mechanisms and Role in Cardiovascular Disease." *International Society of Differentiation* 83(2): 1–29.

Ding, Qianshan et al. 2016. "AGXT2L1 Is Down-Regulated in Heptocellular Carcinoma and Associated with Abnormal Lipogenesis." *Journal of Clinical Pathology* 69(3): 215–20.

Gupta-Agarwal, Swati, Timothy J. Jarome, Jordan Fernandez, and Farah D. Lubin. 2014. "NMDA Receptor- and ERK-Dependent Histone Methylation Changes

in the Lateral Amygdala Bidirectionally Regulate Fear Memory Formation." *Learning and Memory* 21(7): 351–62.

Hansel, Christian et al. 2006. "ACaMKII Is Essential for Cerebellar LTD and Motor Learning." *Neuron* 51(6): 835–43.

Huang, E J, and L F Reichardt. 2001. "Neurotrophins: Roles in Neuronal Development and Function." *Annual review of neuroscience* 24: 677–736. http://www.ncbi.nlm.nih.gov/pubmed/11520916%0Ahttp://www.pubmedcentral.nih.gov/articlerender.fcgi?artid=PMC2758233.

Kang H, and Schuman EM. 1995. "Long-Lasting Neurotrophin-Induced Enhancement of Synaptic Transmission in the Adult Hippocampus." *Science* 267(March): 1658e1662.

Kim, Ji-Young et al. 2012. "KDM3B Is the H3K9 Demethylase Involved in Transcriptional Activation of Lmo2 in Leukemia." *Molecular and cellular biology* 32(14): 2917–33. http://www.pubmedcentral.nih.gov/articlerender.fcgi?artid=3416203&tool=pmcentrez&rendertype=abstract.

Kim, Sang Jeong et al. 2017. "Long-Term Depression of Intrinsic Excitability Accompanied by Synaptic Depression in Cerebellar Purkinje Cells." *The Journal of Neuroscience* 37(23): 5659–69.

Lachner, M. et al. 2001. "Methylation of Histone H3 Lysine 9 Creates a Binding Site for HP1 Proteins." *Nature* 410(6824): 116–20.

Langmoen, Iver A., and Michael L.J. Apuzzo. 2007. "THE BRAIN ON ITSELF: NOBEL LAUREATES AND THE HISTORY OF FUNDAMENTAL NERVOUS SYSTEM FUNCTION." *NEUROSURGERY* 61(5): 891–908.

Levine, Eric S., Cheryl F. Dreyfus, Ira B. Black, and Plummer Mark R. 1995. "Brain-Derived Neurotrophic Factor Rapidly Enhances Synaptic Transmission in Hippocampal Neurons via Postsynaptic Tyrosine Kinase Receptors." *Proc. Natl. Acad. Sci. USA* 92(August): 8074–77.

Liu, Bao Hua, Andrew D. Huberman, and Massimo Scanziani. 2016. "Cortico-

Fugal Output from Visual Cortex Promotes Plasticity of Innate Motor Behaviour." *Nature* 538(7625): 383–87.

Lohof, Ann M., Nancy Y. Ip, and Mu Ming Poo. 1993. "Potentiation of Developing Neuromuscular Synapses by the Neurotrophins NT-3 and BDNF." *Nature* 363(6427): 350–53.

Lu, Christian, and Robert C Malenka. 2012. "NMDA Receptor-Dependent Long-Term Potentiation and Long-Term Depression (LTP/LTD)." *Cold Spring Harbor Perspectives in Biology* 4(a005710): 1–15. papers3://publication/uuid/2B3CCE4A-7D33-49F8-BD49-A023EB42F767.

Mahamdallie, Shazia et al. 2019. "Identification of New Wilms Tumour Predisposition Genes : An Exome Sequencing Study." 3(May).

Okamoto, Takehito et al. 2011. "Post-Training Cerebellar Cortical Activity Plays an Important Role for Consolidation of Memory of Cerebellum-Dependent Motor Learning." *Neuroscience Letters* 504(1): 53–56. http://dx.doi.org/10.1016/j.neulet.2011.08.056.

Phillips, Joseph R., Doaa H. Hewedi, Abeer M. Eissa, and Ahmed A. Moustafa. 2015. "The Cerebellum and Psychiatric Disorders." *Frontiers in Public Health* 3(66): 1–8. http://www.frontiersin.org/Child_Health_and_Human_Development/10.3389/fpubh.2015.00066/abstract.

Rambold, H et al. 2002. "Partial Ablations of the Flocculus and Ventral Paraflocculus in Monkeys Cause Linked Deficits in Smooth Pursuit Eye Movements and Adaptive Modification of the VOR." *J Neurophysiol* 87(2): 912–24.

Riessland, Markus et al. 2017. "Neurocalcin Delta Suppression Protects against Spinal Muscular Atrophy in Humans and across Species by Restoring Impaired Endocytosis." *American Journal of Human Genetics* 100(2): 297–315.

Rieubland, Sarah, Arnd Roth, and Michael Hausser. 2014. "Structured

Connectivity in Cerebellar Inhibitory Networks." *Neuron* 81: 913–29.

Ryu, Changhyeon et al. 2017. " STIM1 Regulates Somatic Ca 2+ Signals and Intrinsic Firing Properties of Cerebellar Purkinje Neurons ." *The Journal of Neuroscience* 37(37): 8876–94.

Sadakata, Tetsushi et al. 2014. "Axonal Localization of Ca 2 + -Dependent Activator Protein for Secretion 2 Is Critical for Subcellular Locality of Brain-Derived Neurotrophic Factor and Neurotrophin-3 Release Affecting Proper Development of Postnatal Mouse Cerebellum." 9(6): 1–10.

Scharf, Matthew T. et al. 2017. "Protein Synthesis Is Required for the Enhancement of Long-Term Potentiation and Long-Term Memory by Spaced Training." *Journal of Neurophysiology* 87(6): 2770–77.

Segal, A, I Scott, L Pomeroy, and D Stiles. 1995. "Axonal Growth and Fasciculation Linked to Differential Expression of BDNF and NT3 Receptors in Developing Cerebellar Granule Cells GPDH Gr Cb." *The Journal of Neuroscience* 15(July): 4970–81.

Shao, Ling, and Marquis P. Vawter. 2008. "Shared Gene Expression Alterations in Schizophrenia and Bipolar Disorder." *Biological Psychiatry* 64(2): 89–97.

Upadhyay, Aaradhita et al. 2019. "Neurocalcin Delta Impairs Adult Neurogenesis Whereas Half Reduction Is Not Pathological." *Frontiers in Molecular Neuroscience* 12(February): 1–15.

Waggener, C. T., J. L. Dupree, Y. Elgersma, and B. Fuss. 2013. "CaMKII Regulates Oligodendrocyte Maturation and CNS Myelination." *Journal of Neuroscience* 33(25): 10453–58.

Wan, Guoqiang et al. 2014. "Neurotrophin-3 Regulates Ribbon Synapse Density in the Cochlea and Induces Synapse Regeneration after Acoustic Trauma." *eLife* 2014–Octob: 1–35.

Whitton, Laura et al. 2016. "Cognitive Analysis of Schizophrenia Risk Genes That Function as Epigenetic Regulators of Gene Expression." *American journal of medical genetics* 171B(October): 1170–79.

Xu, Ming, and Elizabeth M Sajdel-sulkowska. 2013. “Aberrant Cerebellar Neurotrophin-3 Expression Induced by Lipopolysaccharide Exposure During Brain Development.” : 316–18.

Yamatani, Hitoshi et al. 2010. “Proteomics Analysis of the Temporal Changes in Axonal Proteins during Maturation.” *Developmental Neurobiology* 70(7): 523–37.